Dealumination of Faujasite, Mazzite, and Offretite with Ammonium Hexafluorosilicate

BRIGITTE CHAUVIN,* MARC BOULET,* PASCALE MASSIANI,* FRANÇOIS FAJULA,*,[1]
FRANÇOIS FIGUERAS,* AND THIERRY DES COURIÈRES†

*Laboratoire de Chimie Organique Physique et Cinétique Chimique Appliquées, U.R A. 418 du C.N.R.S.,
8 Rue de l'Ecole Normale, 34053 Montpellier Cédex 1, France and †Centre de Recherche ELF FRANCE,
B.P. 20, 69360 Saint Symphorien d'Ozon, France

Synthetic faujasite, mazzite, and offretite have been dealuminated with ammonium hexafluorosilicate. The products have been characterized by elemental analysis, X-ray diffraction, volumetry, scanning electron microscopy, stepwise thermal desorption of ammonia, solid-state NMR and IR spectroscopy. Their catalytic activity has been evaluated using isooctane cracking as test reaction. The maximum level of dealumination which can be achieved without loss of X-ray crystallinity corresponds to 50% for faujasite and 30% for mazzite and offretite. This result and the fact that the dealumination capability depends on the texture of the crystals suggest that the reaction is diffusion controlled. The comparison of the acidic and catalytic properties of the parent and dealuminated samples shows small differences indicating that the fluorosilicate treatment replaces weakly bound and weakly acidic aluminium atoms. © 1990 Academic Press, Inc.

INTRODUCTION

Large-pore silicon-rich zeolites are of interest for catalytic purposes because they combine desirable sieving characteristics with high thermal stability and strong acidity.

Synthetic large-pore zeolites, i.e., zeolites with pores defined by rings of 12 tetrahedra leading to free apertures greater than 0.6 nm, are generally obtained with silicon to aluminum ratios lower than five. This ratio can be increased by hydrothermal or chemical postsynthesis treatments. Among the latter, reactions with mineral acids (1), chelating agents (2), silicon tetrachloride (3), phosgene (4), nitrosyl chloride (5), boron trichloride (6), and ammonium hexafluorosilicate (7, 8) have been reported.

The fluorosilicate method is attractive because it allows one to produce silicon-enriched zeolites which are almost free of framework defects. Moreover, the reaction

is carried out in aqueous media under relatively mild conditions.

The mechanism of the dealumination involves two basic steps (7). Aluminium is extracted first from the framework as a soluble fluoride complex leaving a vacancy in which silicon is inserted in a second step. It has been suggested (9) that aluminium is removed in the form of AlF_6^{3-} ion whereas the inserted species is monomolecular silicic acid $Si(OH)_4$.

The original reports of Breck and Skeels (7, 8) and a more recent study (10) emphasize how critical are the experimental conditions on the properties of the dealuminated products. Actually a proper balance should be found between the rate of aluminium extraction and the rate of silicon insertion in order to avoid structural collapse.

The fluorosilicate dealumination has been successfully applied to a series of synthetic zeolites Y,L,W,ρ, offretite, mordenite, and ferrierite and natural ones such as mordenite, erionite, clinoptilolite and chabazite (7, 8). While Breck and Skeels (8)

[1] To whom correspondence should be addressed.

failed to dealuminate synthetic mazzite (ω) by this procedure, it was claimed recently (*11*) that a mazzite-type zeolite synthesised without organic template could be readily converted into a crystalline silicon-enriched material by treatment with fluorosilicate salts.

This paper describes the physicochemical properties of synthetic faujasite, offretite, and mazzite dealuminated by using the $(NH_4)_2SiF_6$ method. The effect of the treatment on the acidity and the catalytic activity of the final products is emphasized. In addition, the influence of the origin of the parent zeolite has been studied by comparing the behavior of two mazzite samples exhibiting different textural characteristics.

EXPERIMENTAL

1. Parent Zeolites

The original offretite and mazzite samples have been prepared by separating the nucleation and growth steps during synthesis in order to control the final crystal morphologies as described in detail elsewhere (*12–14*). Offretite was synthesized in the presence of potassium and tetramethylammonium (TMA) cations. It appeared as rod-like crystals with an average size of 0.4×1 μm. A first mazzite sample (MAZ(A)) was produced in highly alkaline media using sodium aluminate as aluminium source. It consisted of spherulitic particles (1 to 2 μm) with a rough surface giving them the aspect of aggregates of elongated rods. A second sample (MAZ(B)) was prepared by hydrothermal conversion of kaolinite. Single crystals with hexagonal morphology were obtained with an average size 0.7×3 μm.

The three solids were calcined for 4 h at 773 K in flowing (100 ml/min) dry air in order to decompose the TMA ions, then exchanged for 20 h in 1 M ammonium nitrate at 333 K to produce the ammonium forms. In the case of the offretite sample, the above treatment resulted in a K/Al molar ratio of 0.34. Higher exchange degrees were not looked for in order to preserve the integrity of the crystallinity. The sample was termed

NH$_4$–OFF. The Na/Al ratios obtained with mazzite were 0.04 for sample A (NH$_4$–MAZ(A)) and 0.06 for sample B (NH$_4$–MAZ(B)).

The parent faujasite was an 82% ammonium-exchanged zeolite Y (NH$_4$–Y) obtained from Linde under the reference SK41.

The main physicochemical characteristics of the ammonium-exchanged zeolites used here as starting materials are given in the first columns of Tables 2–7. The morphology of the crystals are shown in Figs. 1–3 and 6.

2. Dealumination Procedure

Dealumination with ammonium hexafluorosilicate has been performed according to the procedure disclosed by Breck and Skeels (*8*). The zeolite was dispersed in water or ammonium acetate solution which was heated to the desired reaction temperature. The $(NH_4)_2SiF_6$ solution was added dropwise while maintaining a vigorous stirring. At the end of the addition the pH was recorded.

After reaction, the hot suspension was filtered to recover the solid product. The zeolite was thoroughly washed (2 liters per gram) with boiling deionized water and oven dried at 383 K overnight. The reaction media and the experimental conditions used are gathered in Table 1. Experiments 1 and 2 in Table 1 correspond to the exact reproduction of examples 2 and 13, respectively, of the patent of Breck and Skeels (*8*).

3. Characterization Studies

The parent and dealuminated zeolites were characterized by X-ray diffraction (XRD) (crystallinity, purity, cell parameters), scanning electron microscopy (SEM) (morphology), high-resolution solid-state NMR spectroscopy (^{29}Si NMR, framework Si/Al ratios), infrared (IR) spectroscopy (framework vibrations), and elemental analysis (EA). Details of the procedures have been published previously (*15*).

Prior to the studies of sorption, acidity, and catalysis the solids were calcined in

TABLE 1

Experimental Conditions for the Fluorosilicate Treatments

Experiment	Zeolite	Reaction medium[a]	A.F.S.[b] sol.	SiF$_6$/ Al	Rate of addition	pH	Reaction	
							Temperature (K)	Time (h)
1	NH$_4$–Y; 2 g	3.4 Molar A.A. 100 ml, 348 K	0.089 M, 50 ml	0.5	2 ml/5 min	6.5	348	18
2	NH$_4$–OFF; 5 g	100 ml H$_2$O 368 K	0.14 M, 50 ml	0.38	2 ml/5 min	4.5	368	3
3	NH$_4$–MAZ(A); 2 g	2 Molar A.A., 150 ml, 358 K	0.06 M, 50 ml	0.39	1 ml/5 min	5.5	358	3
4	NH$_4$–MAZ(A); 0.52 g	2 Molar A.A., 50 ml, 368 K	0.152 M, 10 ml	0.75	1 ml/5 min	6.5	368	3
5	NH$_4$–MAZ(A); 0.7 g	3.4 Molar A.A., 90 ml, 350 K	0.52 M, 10 ml	1.9	1 ml/5 min	7	350	18
6	NH$_4$–MAZ(B); 2 g	40 ml H$_2$O, 368 K	0.14 M, 20 ml	0.35	2 ml/5 min	5	368	3

[a] A.A.: Ammonium acetate solution.
[b] A.F.S.: Ammonium fluorosilicate.

flowing dry air at 773 K for 4 h and again characterized by XRD, ^{29}Si NMR, and IR.

Hydrocarbon and water sorption capacities at $P/P_0 = 0.2$ and 0.9 and nitrogen pore volumes were determined by gravimetry and volumetry, respectively (16). Stepwise thermal desorption (STD) of ammonia was used to measure the acidity of the calcined solids. The zeolite sample (100 mg) was placed in a quartz reactor and dehydrated at 873 K for 4 h under flowing nitrogen. The reactor temperature was then decreased to 373 K and the zeolite saturated with ammonia for 2 h. The excess of base was evacuated by pumping the system to 10^{-3} Torr (1 Torr = 133.3 N m^{-2}). The nitrogen flow was restored and the temperature was increased (1 K min^{-1}) stepwise to 873 K (steps of 50 K, time of each plateau 40 min, except at 873 K where the plateau lasted 2 h). The ammonia evolved was trapped in a HCl solution of known composition which was continuously titrated by conductimetry. This method allowed for an accurate and reproducible measure of the strong acid sites present at the surface of the solids.

The catalytic activity was evaluated for isooctane (2,2,4-trimethylpentane) cracking at 653 K in nitrogen (N$_2$/hydrocarbon = 60) in a fixed-bed continuous flow microreactor connected to a GPC analytical device. The zeolite (20 to 40 mg) was mixed with 80 to 60 mg of catalytically inactive alumina. Space velocities were adjusted in order to compare all solids in the range of 5 to 10% of total conversion.

TABLE 2

Properties of NH$_4$–Y and of the Product Treated with Fluorosilicate

	NH$_4$–Y	NH$_4$Y–FS
Na$_2$O wt%	2.5	0.8
(NH$_4$)$_2$O wt%	9.8	5.8
Al$_2$O$_3$ wt%	22.3	12.9
SiO$_2$ wt%	64.9	80.5
F$_2$ wt%		0.1
Si/Al molar (E.A.)[a]	2.47	5.3
Si/Al molar (NMR)[b]	2.55	5.0
Na/Al molar	0.18	0.10
total cations/Al	1.04	1.04
% crystallinity	100	109
a_0 (A)	24.76	24.52

[a] Derived from elemental analysis.
[b] Framework silica to alumina ratio obtained by ^{29}Si NMR spectroscopy.
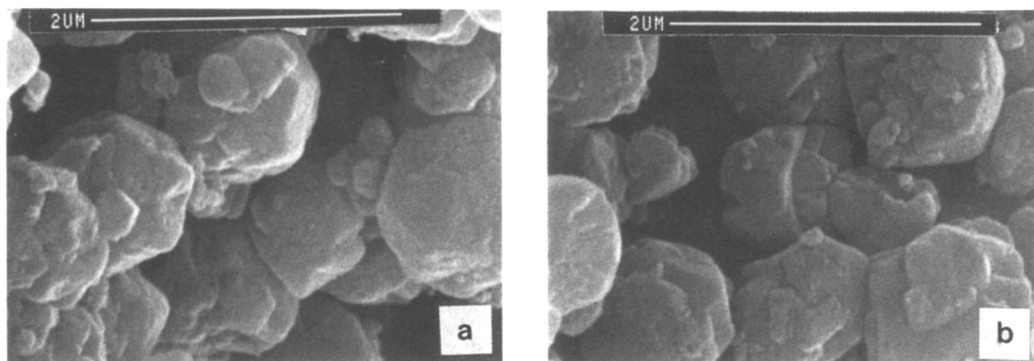
FIG. 1. Scanning electron micrographs of (a) NH_4–Y and (b) NH_4–Y–FS.

RESULTS AND DISCUSSION

1. Influence of Dealumination on the Chemical Composition and Crystallinity

The physicochemical characteristics of the various starting and dealuminated zeolites are given in Tables 2–7. Whenever possible, equivalent data available from the literature have been reported for comparison.

Faujasite. The fluorosilicate treatment produced a highly crystalline product with a contracted unit cell (u.c.) and a framework silicon to aluminium ratio derived from ^{29}Si NMR very similar to that calculated from the elemental analysis (Table 2). The texture of the crystals (Fig. 1b) was not modified and the zeolite was thermally stable when heated at 773 K.

According to the reaction stoechiometry in experiment 1 (Table 1), the maximum amount of aluminium extractible with the quantity of $(NH_4)_2SiF_6$ present would correspond to 27 Al/u.c. (50% of dealumination). The value actually found in sample NH_4–Y–FS was 25 Al extracted per u.c. All these results agree well with those reported and discussed by Breck and Skeels (8) and Garralon *et al.* (10).

Offretite. The elemental analysis of NH_4–OFF–FS (Table 3) shows that the reaction led, as expected, to an increase of the silicon to aluminium ratio and a decrease of the potassium equivalent content. The value of the framework silicon to aluminium ratio,

lower than that obtained by elemental analysis, the significant quantity of fluoride found on the solid, and the roughness of the surface of the crystals (Fig. 2b) all argue for the presence of residual silicate on the crystallites despite their extensive washing by boiling water. The zeolite was highly crystalline after calcination in air at 773 K but no longer sorbed cyclohexane (Table 4) whereas the water and *n*-hexane sorption capacities remained high. These measurements suggest the formation of a surface silica layer which would reduce the aperture of the channels but would leave intact the intracrystalline void space.

Taking into account the silicon to aluminium ratio measured by NMR we conclude that 1.1 aluminium atom has been extracted per unit cell (25% of dealumination) whereas the amount of fluorosilicate in the reaction medium had been designed in order to extract 1.6 Al/u.c. With the low degree of dealumination achieved no evidence for substantial changes in the unit cell dimensions could be found. The use of harder experimental conditions (18 h of reaction or $(NH_4)_2SiF_6$/Al molar ratios of 0.5 and 0.75) produced materials with XRD crystallinities lower than 30%.

The last two columns of Table 3 report the data of example 13 of the patent of Breck and Skeels (8). In this experiment the molar ratio $(NH_4)_2SiF_6$/Al was 0.51 and the zeolite was digested for 3 h at 368 K. By using a

CHAUVIN ET AL.

TABLE 3

Properties of NH$_4$–OFF and of the Product Treated with Fluorosilicate
(Comparison with Data of Breck and Skeels (8))

	This work		Ref. (8)	
	NH$_4$–OFF	NH$_4$–OFF–FS	NH$_4$–OFF	NH$_4$–OFF–FS
K$_2$O wt%	5.87	2.39	2.48	1.47
(NH$_4$)$_2$O wt%	5.50	4.20	5.31	2.72
Al$_2$O$_3$ wt%	18.56	13.10	14.05	8.27
SiO$_2$ wt%	69.76	80.21	76.15	84.71
F$_2$ wt%		0.23		0.12
Si/Al molar (E.A.)^a	3.20	5.20	4.60	8.69
Si/Al molar (NMR)^b	3.20	4.5	—	—
K/Al molar	0.34	0.20	0.19	0.19
total cations/Al	0.92	0.83	0.93	0.83
% crystallinity	100	95	100	60
a_0 (A)	13.22	13.21	—	—
c_0 (A)	7.55	7.54	—	—

^{a} See footnote a in Table 2.
^{b} See footnote b in Table 2.

starting material which was already silicon-enriched and containing less potassium than our sample, the reaction led to 42% of dealumination but the product was only 60% crystalline.

Mazzite (sample A). Figure 3 shows the macroscopic aspect of the parent NH$_4$–MAZ(A) and of the products obtained in experiments 4 and 5 (Table 1). The corresponding XRD spectra are given in Fig. 4. (The product obtained in experiment 3 had nearly identical properties than that of ex-periment 4, so data are not presented). For the fluorosilicate-treated zeolites the individual elongated rods on the surface of the spheroids and the spheres themselves appeared as melted together. The XRD peaks were still narrow and intense but a broad background developed in the region of 8 to 20°. The data of Table 5 indicate that in both cases the level of dealumination was very low (less than 15%) and that the solids contained significant amounts of silicate impurities (bulk silicon to aluminium ratios larger
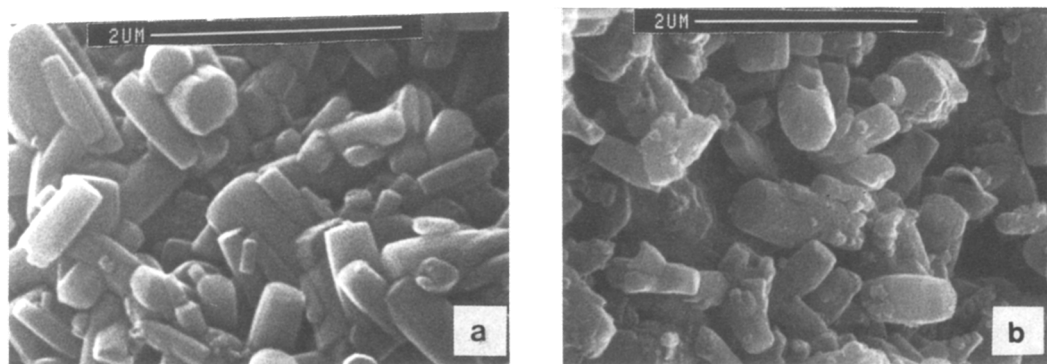

FIG. 2. Scanning electron micrographs of (a) NH$_4$–OFF and (b) NH$_4$–OFF–FS.

TABLE 4

Hydrocarbon and Water Sorption Capacities
(in ml g^{-1}) of the Parent and Dealuminated Offretite

Sorbate sample	Water P/P_0		n-Hexane P/P_0		Cyclohexane P/P_0	
	0.2	0.9	0.2	0.9	0.2	0.9
NH$_4$–Y	0.21	—	0.12	0.13	0.09	0.10
NH$_4$–Y–FS	0.19	—	0.10	0.12	<0.01	0.01

Note. The solids have been calcined at 773 K in air prior to the measurements.

than framework ratios, presence of fluoride, increase of the total cation to aluminium ratio). These impurities were nevertheless not detected in the XRD spectra.

When the samples were calcined in air at 773 K, a significant loss of crystallinity was observed (Fig. 5). In order to better describe the texture of the various solids, hydrocarbon and water sorption capacities were measured at 298 K by gravimetry. As has been discussed previously (*16*), the sorption capacities determined at $P/P_0 = 0.2$ represent a measure of the available intracrystalline void volume and the values determined at $P/P_0 = 0.9$ a measure of the total pore volume (micropores plus mesopores plus external surface). The results show (Table 6) that both the microporous and total volumes available to the sorbents were severely reduced after reaction. The decrease of sorption capacity was greater the larger the kinetic diameter of the sorbed molecule. All these facts suggest that under our conditions of treatment, the fluorosilicate salt has been trapped on the rough mesoporous surface of the particles and reacted essentially with the outer part of the crystallites. This would result in the formation of a silicate layer coating the crystals and preventing the access of the structural porosity to the reagents. Little, if any, dealumination then occurred. Upon calcination the surface silicate would transform into silica, blocking the porosity of the zeolite.

Mazzite (sample B). When the fluorosilicate treatment was performed on the hexag-

onal crystals of mazzite (Fig. 6) under the conditions corresponding to experiment 6 in Table 1, a highly crystalline solid (Fig. 7), 30% enriched in silicon, was obtained. In the infrared spectrum of the framework re-
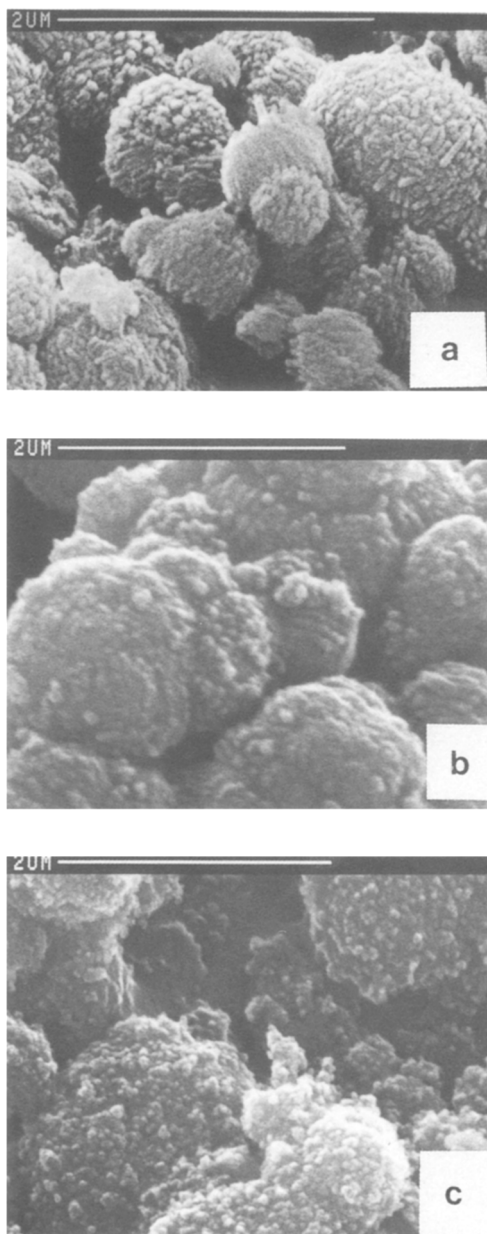

FIG. 3. Scanning electron micrographs of (a) NH$_4$–MAZ(A), (b) NH$_4$–MAZ(A)FS obtained in experiment 4, and (c) NH$_4$–MAZ(A)FS obtained in experiment 5.
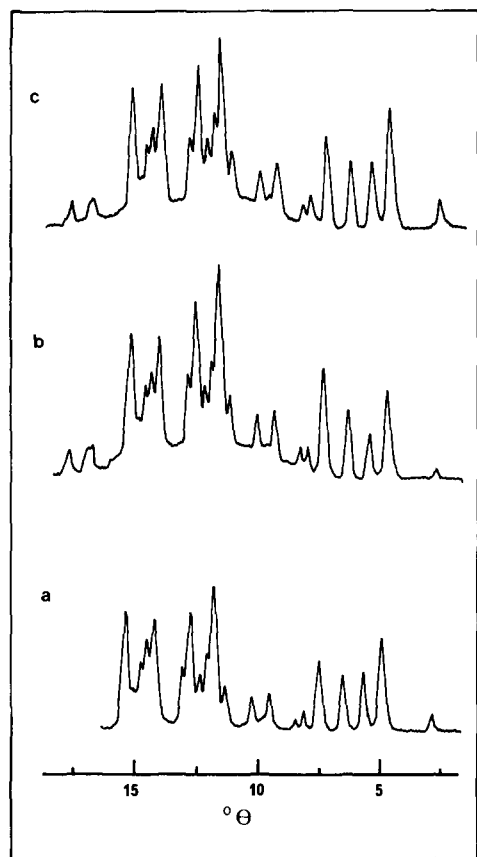
CHAUVIN ET AL.

FIG. 4. X-ray diffractograms of (a) NH₄–MAZ(A), (b) NH₄–MAZ(A)FS obtained in experiment 4, and (c) NH₄–MAZ(A)FS obtained in experiment 5.

TABLE 5

Properties of NH_4–MAZ (A) and of the NH_4–MAZ(A)–FS Products Obtained in Experiments 4 and 5

	NH_4–MAZ(A)	NH_4–MAZ(A)–FS	
		Exp. 4	Exp. 5
Na_2O wt%	0.5	0.37	0.16
$(NH_4)_2O$ wt%	8.42	7.69	6.91
Al_2O_3 wt%	19.06	15.76	12.15
SiO_2 wt%	71.71	74.88	77.94
F_2 wt%		1.16	2.80
Si/Al molar (E.A.)[a]	3.2	4.03	5.45
Si/Al molar (NMR)[b]	3.3	3.6	4.05
total cations/Al	0.90	0.99	1.12
% crystallinity	100	70	65

[a] See footnote a in Table 2.
[b] See footnote b in Table 2.

fluorosilicate method is the patent by Cannan (11). His data, given for comparison in Table 7, indicate a level of dealumination of 35% accompanied by a discrete loss of crystallinity.

2. Influence of Dealumination on the Acidity and Catalytic Activity

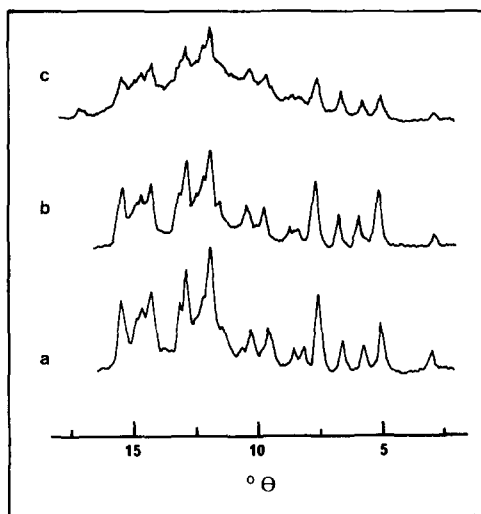The results of the stepwise thermal desorption (STD) experiments are given in

gion all bands were shifted to higher frequencies (Fig. 7) but no significant changes in the unit cell parameters were noticed. The low residual content in fluoride and the identical values of the silicon to aluminium ratios found for the bulk and for the framework (Table 7) indicate that the zeolite was almost free of silicate or aluminate impurities. However, the sorption measurements revealed a loss in sorption capacity (Table 6, last entries) suggesting some pore blocking by silicate. The effect was less pronounced than with sample A and corresponded to a reduction of 25 and 50% of the volumes accessible to n-hexane and 1,3,5-trimethylbenzene, respectively.

To our knowledge the only report on the successful dealumination of mazzite by the

FIG. 5. Influence of the calcination at 773 K in air on the XRD crystallinity of (a) NH₄–MAZ(A), (b) NH₄–MAZ(A)FS experiment 4, and (c) NH₄–MAZ(A)FS experiment 5.

TABLE 6

Hydrocarbon and Water Sorption Capacities (in ml g^{-1}) of the Parent and Dealuminated Mazzite Samples

Sorbate	Water P/P_0		n-hexane P/P_0		1,3,5-trimethylbenzene	
Sample	0.2	0.9	0.2	0.9	0.2	0.9
NH$_4$–MAZ (A)	0.080	0.190	0.061	0.121	0.051	0.110
NH$_4$–MAZ (A) FS 4	0.075	0.174	0.017	0.062	<0.01	0.024
NH$_4$–MAZ (A) FS 5	0.061	0.126	0.020	0.048	<0.01	0.020
NH$_4$–MAZ (B)	0.099	0.110	0.077	0.080	0.064	0.066
NH$_4$–MAZ (B) FS	0.082	0.10	0.060	0.065	0.031	0.035

Note. All the solids have been calcined at 773 K in air prior the measurements.

Fig. 8 and Table 8. The exposure of NH$_3$ at elevated temperature (373 K) followed by evacuation at the same temperature suppresses the physical adsorption and minimizes the weakly bound NH$_3$. The amounts of NH$_3$ desorbed here may then be considered as a measure of the distribution and number of strong acid sites of the solids. Using this criterion we can see from Table 8 that nearly 50% and less than 30% of the protonic centers can be considered as strongly acidic in the parent FAU and OFF and MAZ(B), respectively. The small quantity of strong sites found on the two latter zeolites results; not only from the presence of weak acid sites but also from the fact that strong acid sites may be located in cages or cavities not accessible to the base. Although

the temperature peak maxima should not be used for comparison of the acid strengths of zeolites with different structures (*17*), the data of Fig. 8 suggest the presence of stronger sites on offretite and mazzite than on faujasite, in agreement with previous studies (*18–20*).

After the dealumination treatment, the acidity of the three zeolites was modified in different ways.

On faujasite, the relative percentage of strongly acidic sites was increased to 70%, but their absolute amount and the distribution of their strengths were not greatly affected. This indicates that the substitution of aluminium by silicon occurred essentially at sites associated with a weak acidity. This result parallels the observations made using
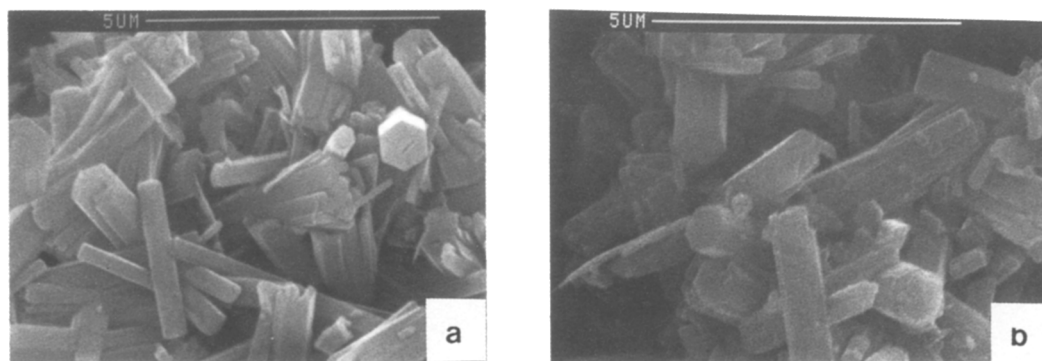

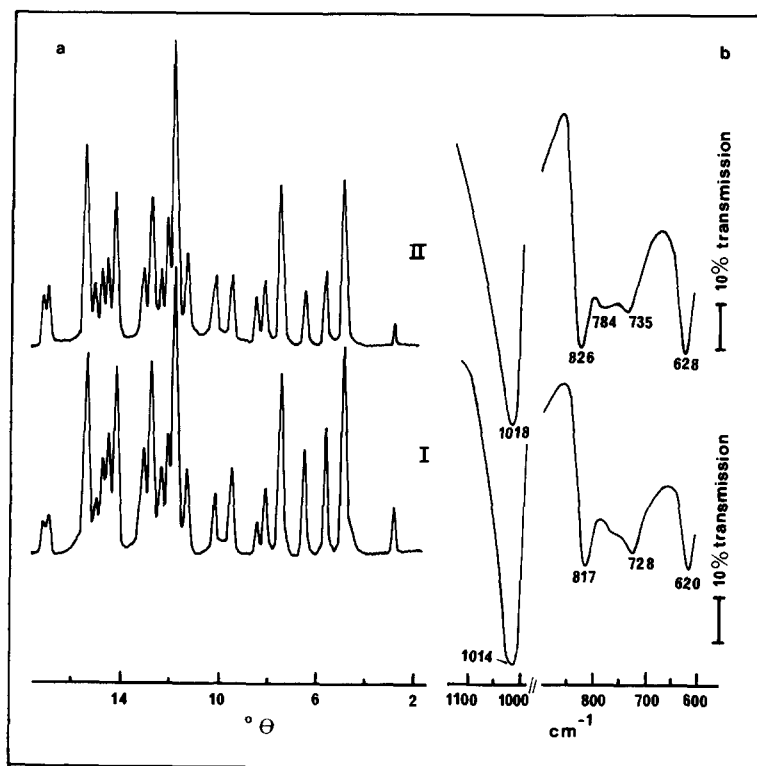FIG. 6. Scanning electron micrographs of (a) NH$_4$–MAZ(B) and (b) NH$_4$–MAZ(B)FS.

CHAUVIN ET AL.

FIG. 7. XRD spectra (a) and IR spectra of the framework region (b) of NH_4-MAZ(B) before (I) and after (II) the fluorosilicate treatment.

TABLE 7

Properties of NH_4–MAZ (B) and of the Product Treated with Fluorosilicate
(Comparison with Data of Cannan (11))

	This work		Ref. (11)	
	NH_4–MAZ(B)	NH_4–MAZ(B)–FS	NH_4–MAZ	NH_4–MAZ–FS
Na_2O wt%	0.71	0.48	0.25	0.20
$(NH_4)_2O$ wt%	7.17	5.00	8.06	5.24
Al_2O_3 wt%	20.04	14.42	19.76	13.04
SiO_2 wt%	12.08	78.86	71.91	81.5
F_2 wt%		0.14		—
Si/Al molar (E.A.)[a]	3.05	4.65	3.09	5.3
Si/Al molar (NMR)[b]	3.2	4.60	—	—
total cation/Al	0.76	0.70	0.82	0.81
% crystallinity	100	100	100	75–85
a_0 (A)	18.23	18.23	—	—
c_0 (A)	7.62	7.61	—	—
VN_2 (ml/g)[c]	0.079	0.081	—	—

[a] See footnote a in Table 2.
[b] See footnote b in Table 2.
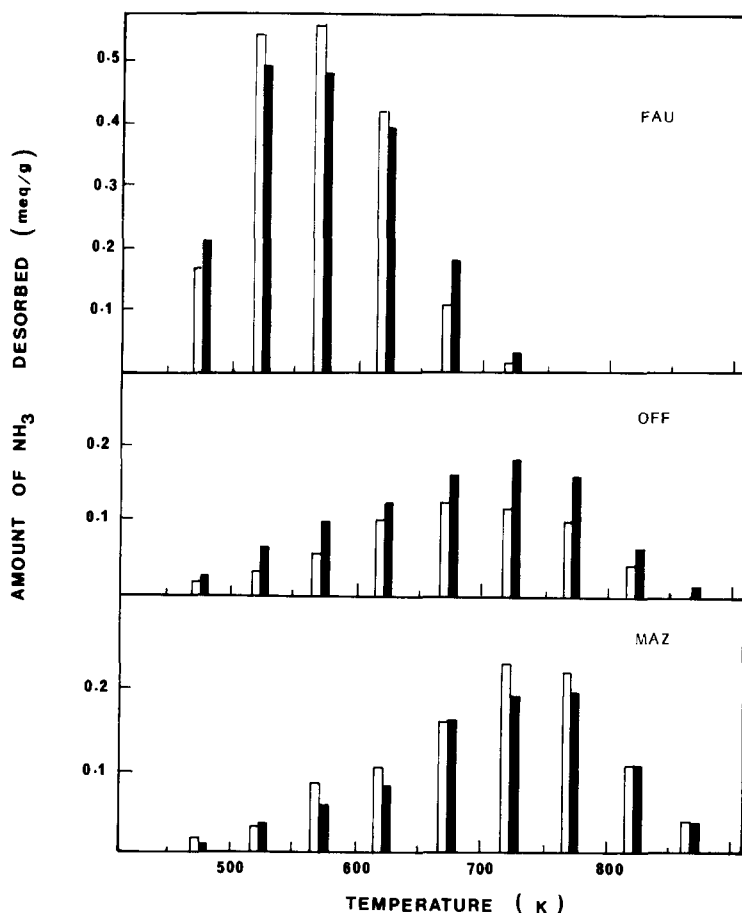[c] Nitrogen microporous volume after calcination at 773 K.

FIG. 8. Acidity distributions determined by stepwise thermal desorption of ammonia. Open bars: before the SiF_6 treatment. Solid bars: after dealumination.

other dealumination methods which show that the removal of the first 30 aluminium atoms per unit cell has little effect on the strong acidity of faujasite (21, 22).

On offretite, the absolute and relative number of acid sites were both increased; the effect was particularly pronounced for the sites desorbing ammonia at a temperature higher than 673 K. This can be interpreted by a selective replacement of weakly bound (and weakly acidic) Al centers and the decrease of the K/Al ratio (23).

Finally, the dealuminated mazzite contained fewer acid centers than the parent zeolite, but the distribution of sites was only barely modified by the treatment.

The variation of the rate of isooctane cracking at 653 K as a function of the time on stream is reported in Figs. 9 and 10 for the three parent and dealuminated zeolites. Catalysts derived from faujasite exhibited a much better stability of the activity than those prepared from offretite and mazzite. The initial activity of the offretite samples, before and after dealumination, was comparable to that of the faujasite solids. The catalytic test reaction did not therefore reflect the difference in acidity evidenced in the STD experiments, suggesting that the level of activity was more determined by configurational limitation (the FAU structure has a tridirectionnal network of large pores

TABLE 8

Amounts of NH_3 Desorbed in the STD Experiments and Theoretical Number of Acid Sites of the Various Solids

Zeolite	FAU		OFF		MAZ(B)	
	Parent	Dealuminated	Parent	Dealuminated	Parent	Dealuminated
NH_3 desorbed (meq g^{-1})	1.71	1.57	0.61	0.83	1.03	0.90
H^+ theor.[a] (meq g^{-1})	3.58	2.23	2.35	2.02	3.65	2.76
% sites	47.8	70.4	26	41	28	32

[a] Calculated from the aluminium content and taking into account the residual cation content.

whereas OFF behaves as a unidirectional sieve with respect to isooctane) than by the density and strength of the acid sites. This point has already been discussed by Bourdillon et al. (19) who found that offretite was six times more active than faujasite in n-hexane cracking but only one-half as active in ortho-xylene isomerization. The mazzite catalysts were apparently the most active initially but the very fast activity decay did not permit an accurate determination of initial reaction rates.

As a general rule, the fluorosilicate treatment resulted, for all the zeolites, in a slight increase of the activity but had no influence on the deactivation characteristics. The reaction products consisted of C_3 to C_5 hydrocarbons with the C_4 fraction representing 80–90% molar (iso-C_4/n-C_4 = 8 − 10). The C_3/C_5 ratio was close to 1 on FAU and was equal to 1.3 and 1.6 on OFF and MAZ, respectively. These values varied little upon deactivation and dealumination. The initial isobutene/isobutane ratios were increased after dealumination (from 0.2 to 0.4 on FAU, from 0.5 to 0.65 on OFF, and from
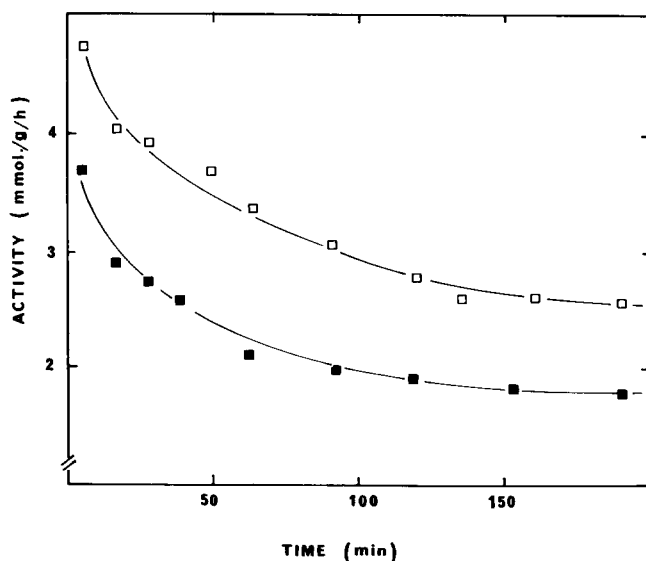
FIG. 9. Activity of ■ NH_4–FAU and □ NH_4–FAU–FS for isooctane cracking at 653 K.
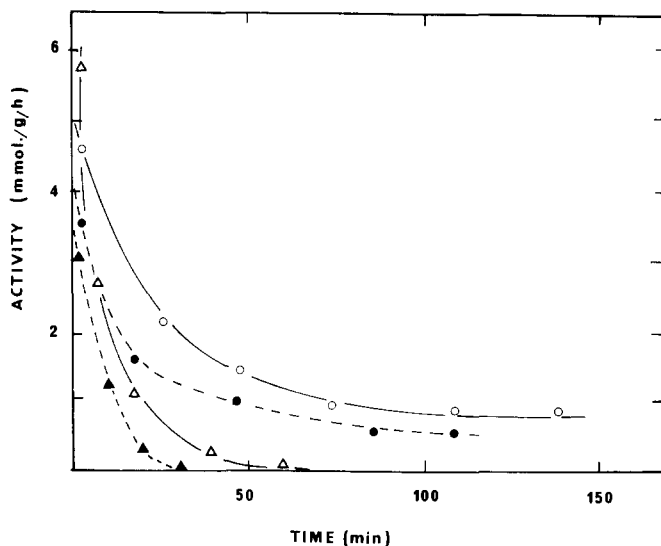
FIG. 10. Activity of NH$_4$-MAZ(B) (▲ before and △ after SiF$_6$ dealumination) and of NH$_4$-OFF (● before and ○ after SiF$_6$ dealumination) for isooctane cracking at 653 K.

0.4 to 0.7 on MAZ) but this difference between the parent and dealuminated solids was no longer observed after some time on stream. Thus this ratio equalled 0.6 on FAU and 0.9 on OFF after 2 hours and was near to 1 on MAZ after 20 min under our conditions. The isobutene/isobutane ratio was therefore more dependent on the structural type than on aluminium content.

3. Limitation of the Dealumination in Mazzite and Offretite

The mechanism of dealumination by the ammonium fluorosilicate method implies that the rate of aluminium extraction must not be much higher than the rate of silicon insertion (7–10). In effect, if too many aluminium atoms are extracted from the framework before silicon atoms are inserted, the structure collapses as is the case when dealumination is performed, for example, by mineral acids (24) or chelating agents (21, 25).

This work, and previous studies referred to above, suggest the existence of an optimum level of dealumination without loss of crystallinity corresponding to 50% dealumi-

nation for faujasite and near 30% for offretite and mazzite. The case of faujasite has already been discussed by Garralon et al. (10). The authors demonstrated that after removing ca. 30 aluminium atoms per unit cell, not all the vacancies left by the extracted Al were replaced by Si. Defects were thus created, resulting in loss of crystallinity. For offretite and mazzite, the limit is definitely lower. Since the parent solids had aluminium contents not very far from those found on faujasites, the reasons for the observed difference must stand in the structural and sorption characteristics of the sieves.

The pores in mazzite consist of tubular channels, running parallel to the c crystallographic axis, bounded by twelve-ring apertures with a free diameter of 0.75 nm and walled by chains of four and five rings (26, 27). Offretite also presents rectilinear cylindrical channels parallel to c, with a free diameter of 0.67 nm. For highly decationized offretite, these channels may be interconnected through gmelinite cages with apertures in the range 0.36–0.49 nm (28, 29). These channel geometries have two import-

ant implications. First, the only aluminium atoms which can be reached by sorbates or reagents are those pointing toward the main channel (23, 30). These represent roughly 50% of the total Al atoms of the zeolite. Second, the rate of diffusion of the silicon-containing species to be inserted in the vacancies will be severely limited by the presence of the aluminium complexes leaving the dealuminated sites in the unidirectional channels. The hypothesis that the diffusion of the various species plays an important role in the reaction is supported by the contrasted results obtained with the two mazzite samples. The fluorosilicate treatment was totally inefficient with the rough spherulites whereas it was successful with the prismatic crystals. We have shown recently (16) that the diffusion rates for hydrocarbons were two orders of magnitude smaller on the former than on the latter. The low thermal stability of the spherulitic crystals and the existence of surface barriers were put forward to account for this result.

CONCLUSIONS

The optimum level of dealumination which can be reached by using the fluorosilicate method disclosed by Breck and Skeels (7, 8) while preserving the full crystallinity of the zeolite depends not only on the structural type of the sieve but also on the texture of the parent crystals. This optimum is around 30% dealumination for mazzite and offretite and around 50% for faujasite. Under the conditions of the reaction, the rates of aluminium evacuation and of silicon insertion would be controlled by diffusion, making difficult the adjustment of the variables that could lead to a proper balance between the two processes.

As has been observed many times during dealumination, the removal of a limited number of aluminium atoms has little influence on the distribution of the strong acid sites, indicating that weakly bound (and weakly acidic) aluminium atoms are replaced first.

Using isooctane cracking as test reaction we found that the treatment had a positive effect on the initial activity of the catalysts whereas the deactivation characteristics and product distributions were little modified.

REFERENCES

1. Barrer, R. M., and Coughlan, B., in "Molecular Sieves," p. 141. Society of Chemical Industry, London, 1968.
2. Kerr, G. T., J. Phys. Chem. 71, 4155 (1967).
3. Beyer, H. K., and Belenykaja, I., Stud. Surf. Sci. Catal. 5, 203 (1980).
4. Fejes, P., Kiricsi, I., Hannus, I., and Schöbel, Gy., Stud. Surf. Sci. Catal. 24, 263 (1985).
5. Fejes, P., Schöbel, Gy., Kiricsi, I., and Hannus, I., Acta Phys. Chem., Szeged 31, 119 (1985).
6. Derouane, E. G., Baltusis, L., Dessau, R. M., and Schmitt, K. D., Stud. Surf. Sci. Catal. 10, 305 (1985).
7. Breck, D. W., and Skeels, G. W., "Proceedings, 6th International Zeolite Conf. Reno, 1983" (D. Olson, and A. Bisio, Eds.), p. 87. Butterworths, Guildford, England, 1984.
8. Breck, D. W., and Skeels, G. W., U.S. Patent 4,503,023 (1985).
9. Yigong, H., Caiying, L., and Enze, M., Stud. Surf. Sci. Catal. 49, 189 (1989).
10. Garralon, G., Fornes, V., and Corma, A., Zeolites 8, 268 (1988).
11. Cannan, T. R., Euro-PCT Patent Appl. W087/00158 (1987).
12. Moudafi, L., Dutartre, R., Fajula, F., and Figueras, F., Appl. Catal. 20, 189 (1986).
13. Nicolas, S., Massiani, P., Vera-Pacheco, M., Fajula, F., and Figueras, F., Stud. Surf. Sci. Catal. 37, 115 (1988).
14. Fajula, F., Nicolas, S., Di Renzo, F., Gueguen, C., and Figueras, F., ACS Symp. Ser. 398, 493 (1989).
15. Massiani, P., Chauvin, B., Fajula, F., Figueras, F., and Gueguen, C., Appl. Catal. 42, 105 (1988).
16. Chauvin, B., Fajula, F., Figueras, F., Gueguen, C., and Bousquet, J., J. Catal. 111, 94 (1988).
17. Kapustin, G. I., Brueva, T. R., Klyachko, A. L., Beran, S., and Wichterlova, B., Appl. Catal. 42, 239 (1988).
18. Penchev, V., Minchev, Ch., Kanazirev, V., Pencheva, O., Borisova, N., Kosova, L., Lechert, H., and Kacirek, H., Zeolites 3, 249 (1983).

19. Bourdillon, G., Guisnet, M., and Gueguen, C., *Zeolites* **6**, 221 (1986).
20. Whyte, T. W., Jr., Wu, E. L., Kerr, G. T., and Venuto, P. B., *J. Catal.* **20**, 86 (1971).
21. Barthomeuf, D., and Beaumont, R., *C.R. Acad. Sci. Paris Sér. C* **269**, 1345 (1969); *J. Catal.* **30**, 288 (1973).
22. Beaumont, R., and Barthomeuf, D., *J. Catal.* **26**, 249 (1976); *C.R. Acad. Sci. Paris Sér. C* **272**, 363 (1971).
23. Mirodatos, C., and Barthomeuf, D., *J. Catal.* **57**, 136 (1979).
24. Hernandez, F., Ibarra, R., Fajula, F., and Figueras, F., *Acta Phys. Chem., Szeged* **31**, 81 (1985).
25. Kerr, G. T., *J. Phys. Chem.* **72**, 2594 (1968).
26. Galli, E., *Cryst. Struct. Commun.* **3**, 339 (1974).
27. Rinaldi, R., Pluth, J. J. and Smith, J. V., *Acta Crystallogr.* **B31**, 1603 (1975).
28. Gard, J. A., and Tait, J. M., *Acta Crystallogr.* **B28**, 825 (1972).
29. Meier, W. M., and Opson, D. H., *in* "Atlas of Zeolite Structure Types," p. 114. Butterworth, Stoneham, MA (1987).
30. Klinowski, J., Anderson, M. W., and Thomas, J. M. *J. Chem. Soc. Chem. Commun.* **525** (1983).